Statistical tensile strength of Nextel™ 610 and Nextel™ 720 fibers

DAVID M. WILSON

3M Metal Matrix Composites Department, St. Paul, Minnesota 55144-1000

Abstract

The properties of fiber-reinforced composites are dependent not only on the strength of the reinforcement fiber but also the distribution of fiber strength. In this study, the single filament strength of several lots of Nextel™ 610 and Nextel™ 720 Ceramic Fibers was measured. Fracture statistics were correlated with the effects of gauge length and diameter variation, and the Weibull modulus was calculated using several different techniques. It was found that the measured Weibull modulus at a single gauge length did not accurately predict either the gauge length or diameter dependence of tensile strength.

1. Introduction

Two new polycrystalline fibers, Nextel™ 610 and Nextel™ 720 fiber, have recently become commercially available*. Nextel™ 610 fiber is an alpha-alumina fiber with excellent strength and high elastic modulus. Tensile strengths for polycrystalline fibers above 3 GPa had previously only been achieved by SiC fibers. Oxide fibers have superior resistance to oxidation and corrosion in certain environments; because of this, oxide fibers have the potential to produce composites with unique and superior properties. For instance, the high strength

---

* At this time, both types of fiber are experimental products

of Nextel™ 610 fiber has allowed the development of a new generation of aluminum matrix composites which have tensile strength in excess of 1500 MPa [1]. In addition, oxide fibers are produced from aqueous solutions or sols, and are fired in air, which makes them less expensive than SiC fibers. Nextel™ 720 fiber was developed with the goal of maximizing creep resistance. The creep resistance of Nextel™ 720 fiber is higher than other polycrystalline oxide fiber, and allows the fabrication of composites with useful mechanical properties at 1100 C or above. Both Nextel™ 610 and 720 fibers have excellent chemical stability due to their high alumina content and crystalline nature. A summary of the properties of Nextel™ 610 and 720 fiber are given in Table 1. The microstructure and high temperature properties of both fibers have been described previously [2,3,4].

Nextel™ 610 and 720 fibers are specifically targeted as reinforcements for metal and ceramic composites. The strength of metal and ceramic composites is critically dependent on not only the strength but the strength distribution of the reinforcing fiber. Thus, a thorough understanding of fiber mechanical properties is of prime importance. The purpose of this study is to describe the tensile strength and statistical distribution of tensile strength of Nextel™ 610 and 720 fibers.

The statistical variability of the tensile strength of reinforcement fibers is now commonly reported in terms of Weibull modulus. An excellent review of the subject was given by Van der Zwaag [5]. The Weibull modulus is a parameter used to describe the distribution of strength in materials which break at defects according to weakest link statistics. The probability of failure of a material is given by:

$$P = 1 - \exp [-V/V_o(\sigma/\sigma_o)^m] \qquad (1)$$

where: m = Weibull modulus

V = tested volume

σ = failure strength

V_o, σ_o = scaling constants

By rearranging and taking the natural logarithm of both sides of the equation, the following equation is obtained:

$$\ln (\ln(1/1-P)) - \ln V/V_o = m\cdot\ln \sigma - m\cdot\ln \sigma_o \qquad (2)$$

The Weibull modulus, m, is typically determined graphically by one of two methods. For a constant tested volume (gauge length for fibers), Equation 2 is reduced to:

$$\ln(\ln(1/1-P)) = m\cdot\ln \sigma + k \qquad (3)$$

where k is a constant. The Weibull modulus can be determined by plotting ln (ln(1/1-P)) against ln σ. Alternatively, m can be determined from the gauge length dependence of strength. If we hold the fracture probability P constant by measuring mean strength, then Equation 2 reduces to:

$$\ln \sigma = -1/m \ln V + k' \qquad (4)$$

or, alternatively,

$$\sigma_1/\sigma_2 = (V_2/V_1)^{1/m} \qquad (5)$$

Where the strength at tested volumes V_1 and V_2 are σ_1 and σ_2, respectively, and K' is a constant. Since the tested volume is proportional to gauge length, the Weibull modulus m can be determined by plotting mean strength as a function of gauge length. The slope of such a plot is equal to -1/m. This method of measuring Weibull modulus is attractive because the composite designer is interested in the strength of the fiber at the "ineffective length", or length at which the matrix transfers the load to the fiber in shear within the composite. The ineffective length is typically very small, perhaps a few hundred micrometers in most composite systems. Thus, extrapolating the gauge length dependence of strength to short gauge length should produce the most accurate estimation of composite strength.

To consider the effects of fiber diameter, Equation 1 can be expanded to:

$$P = 1 - \exp [-(\pi/4)LD^2/V_o(\sigma/\sigma_o)^m] \quad (6)$$

where D is the fiber diameter and L is gauge length. By an analogous method to Equation 2:

$$\ln (\ln(1/1-P)) = \ln(\pi/4)L/V_o + 2\ln D + m\cdot\ln \sigma - m\cdot\ln \sigma_o \quad (7)$$

Therefore, for a constant gauge length,

$$\ln \sigma = -2/m \ln D + k'' \quad (8)$$

Thus, a graph of $\ln \sigma$ vs. $\ln D$ should have a slope of $-2/m$.

Another useful and simple equation for estimating Weibull modulus is [6]:

$$m = 1.2/CV \quad (9)$$

where CV is coefficient of variation of strength at a single gauge length. This estimation is very accurate for $m > 10$. For instance, for a CV of 0.10, m is estimated to be 12.

2. Experimental Procedure

Single filament strength testing was performed using rubber-faced clamp grips with 25 x 25 mm grip faces. For Nextel™ 610 fiber, this method was found to give higher breaking loads than paper tabs recommended in ASTM-3379-75. The tested gauge length was 25 mm unless otherwise specified, and the strain rate was 0.02/min. In this study, almost no fibers were lost due to breakage during sample mounting and testing. Achieving good alignment of fibers with the grips and load axis was critical to obtaining accurate load values.

During fiber testing, no fiber remained in the gauge length after fracture. It is believed that this resulted from vibrations caused by the release of stored strain energy during fiber fracture. Therefore, fiber diameter was measured on fiber ends removed from the grips after fiber failure. Scanning electron microscopy (SEM) examination (Cambridge 240, Leica-Cambridge, Ltd, Cambridge, England) found that fiber diameter was constant within 0.1 μm down the length of individual fibers within 25 mm length. Thus, fiber diameter in the grips is expected to be equal to the diameter at the point of fracture. In this work, fiber diameter was measured using a Measure-Rite™ image analysis system (Model M25-6002, Dolan-Jenner Industries, Lawrence, MA), attached to a light microscope (Olympus™ BHS, Olympus Corporation, Lake Success, NY) at 1000X magnification. Prior to this study, a number of fiber diameter measurement methods, including unaided optical microscopy, laser diffraction/refraction and vibroscopes were evaluated. Significant variability was found in all in comparison to SEM measurements. The image analysis system was found to provide the most accurate diameter measurements and was also simple to use, a significant factor in minimizing operator fatigue and maintaining measurement accuracy. In this system, fiber ends were measured relative to a round template on a video monitor. Blind, replicate studies were performed to determine measurement accuracy. The image analysis method was repeatable to an average error of <0.1 µm, and the mean difference between testers was also <0.1 µm. In these tests, diameter values measured using this technique were between 0.0 and 0.3 µm less than SEM measurements (standardized relative to an 10 µm SEM calibration grid). The reason for this difference is unknown. The image analysis system was consistently accurate to <0.1 µm in measuring the calibration grid. Thus, reported tensile strength may be as much as 5% higher (~28 MPa) than true values. Diameter measurements correlated to within 1% (0.12 µm) of diameters calculated from measured fiber density and weight per unit length.

In this study, several production lots of fiber were tested. Fibers were taken from several spools throughout each lot to incorporate any possible property variation within the lot in fiber fracture statistics. For each spool tested, the strength of ten single filaments were measured. Using this data, Weibull modulus was calculated using three methods: 1) Weibull plot, or strength distribution, method (Equation 3), 2) Gauge Length method (Equation 4) and 3) Diameter method (Equation 8). For Weibull plots, $P = (i-0.5)/n$ was used to estimate fracture probability, where n is the number of fibers tested and i is the rank of strength for each fiber. This is the most accurate estimator for small sample sizes [7,8].

3. Results

3.1 Classical Weibull Statistical Analysis

Table 2 shows a data series for Nextel™ 610 and 720 fibers. The measured strengths are typical of fibers currently being produced. The mean breaking loads of these lots were 3077 and 1964 MPa, respectively. The strength of Nextel™ 610 fiber is higher, primarily because of its finer grain size. The diameter of Nextel™ 720 fiber is slightly larger, 12.5 μm compared with 11.5 μm for Nextel™ 610 fiber. The coefficient of variation of diameter of both fibers is small, less than 5%. Figure 1 shows the distribution of single filament strength for three lots of Nextel™ 610 fiber. For individual lots, approximately 80% of the fibers broke within 10% of the mean strength, indicating a high degree of consistency between fibers. The data has a sinusoidal form, as expected. Lot A0184 had the highest mean tensile strength of any lot tested to date, 3500 MPa. Lots A0168 and A0180 were more typical, having tensile strength near 3000 MPa. Weibull plots for the three lots of Nextel™ 610 fiber are shown in Figure 2. The calculated Weibull modulus varied between 10.9 and 12.1 for the three lots (Table 3). The data was fitted using the least squares method; the two-parameter Weibull equation fit the data fairly well, although some deviation of from the best-fit line occurred at the high and low strength extremes. The Weibull modulus calculated using the strength distribution technique (Equation 3) for all three lots of fiber was 11-12. The corresponding strength distribution and Weibull plot for Nextel™ 720 fiber is given in Figures 3 and 4. The tensile strength of Nextel™ 720 fiber was less than that of Nextel™ 610 fiber, ranging from 1500 MPa to 2700 MPa. The Weibull modulus for Nextel™ 720 fiber was also less than for Nextel™ 610 fiber, approximately 7.1 and 8.1 for lots A0080 and A0174, respectively (Table 4)

3.2 Gauge Length Effects

The mean tensile strength of four lots of Nextel™ 610 fiber and one lot of Nextel™ 720 fiber as a function of gauge length is given in Figures 5 and 6, respectively. Ten filaments were measured for each data point. For Nextel™ 610 fiber, the scatter in the data was large enough that the mean strength for all four lots was used to calculate Weibull modulus. For both types of fiber, the reduction of strength with increasing gauge length was small. For Nextel™ 610 fiber, mean fiber strength decreased only 10% (from 3080 to 2780 MPa) for a 10-fold increase in gauge length. For some individual lots, the measured tensile strength actually increased with gauge length. This amount of variability was not surprising, since the coefficient of variation in mean tensile strength averaged about 0.1 or 10% for these fibers, equal to the variation in strength over the gauge length tested. Using the mean strength, the Weibull modulus for Nextel™ 610 and Nextel™ 720 fiber were 22 and 26, respectively. This is substantially higher than the Weibull modulus measured from the distribution of tensile strength.

3.3 Diameter Effects

Commercial ceramic fibers do not have a completely uniform diameter throughout all fibers in a bundle or tow. Because diameter varies from fiber to fiber, testing fibers at constant gauge length does not maintain a constant tested volume. The distribution of volumes is proportional to the distribution of fiber diameters.

The natural log of tensile strength as a function of the natural log of fiber diameter for Nextel™ 610 and Nextel™ 720 fiber is plotted in Figures 7 and 8, respectively. As given in Equation 8, the slope of the best fit line is equal to -2/m. For Nextel™ 610 fiber, the Weibull modulus calculated using this data for all three lots was between 2.6 and 4. The scatter in this data was large; however, the trend was very consistent. A large amount of scatter is expected due to the statistical nature of fracture. The trend was also similar for other data not presented here; thus, the result is believed to be reliable despite the scatter. For Nextel™ 720 fiber, the Weibull modulus was 4.0 and 1.6 for lots A0080 and A0174, respectively. For both Nextel™ 610 and 720 fibers, this value was much lower than determined using the other methods. In both cases, the low m indicated a stronger dependence of strength on diameter than the gauge length measurements. Tables 3 and 4 summarize the Weibull modulus results using all analysis methods.

4. Discussion

The tensile strength of Nextel™ 610 fiber is by far the highest strength measured for any polycrystalline oxide fiber. Other commercially available oxide fibers have reported tensile strengths of no more than 2.1 GPa [9]. Early lots of Nextel™ 610 fiber (pre-1993) had tensile strengths near 2.5 GPa, better than other commercial materials, but lower than target properties for MMC reinforcements. Fractography experiments on early versions of Nextel™ 610 fiber identified several types of fracture origins, including internal inclusions caused by both inorganic and organic particulate contamination, surface welding and other surface damage [10]. Process development work targeted the elimination of these flaws as a method of increasing fiber strength. These efforts were successful; improvements in process cleanliness during precursor preparation and improved fiber processing techniques since that time have resulted in significantly increased single filament strength.

The measured Weibull modulus of Nextel™ 720 fiber and especially, Nextel™ 610 fiber was also much higher than most multifilament ceramic fibers. For instance, Weibull moduli for Nicalon are 3-4 [11-13], Fiber FP 4-6 [12-16], Altex 4-6 [17,18], and carbon fibers 3-8 [19-22]. For early lots of Nextel™ 610 fibers, it was also found that the Weibull modulus was below 10 [23]. As process development work eliminated large flaws and increased tensile strength, the Weibull modulus also increased. This is not surprising, since eliminating large flaws from a population of defects will leave only the small flaws remaining. This would narrow the flaw size distribution, resulting in increased Weibull modulus. Fractography experiments also confirmed that flaw size for recent lots was reduced compared with earlier, weaker fibers. The correlation between high fiber strength and high Weibull modulus has been noted previously [5].

The three Weibull modulus measurement techniques investigated in this study produced very different results. For both Nextel™ 610 and Nextel™ 720 fibers, the calculated Weibull modulus was much higher with the gauge length method than with the Weibull plot method, which was in turn much higher than the diameter method. Thus, it is clear that the simple two-parameter Weibull model does not describe the tensile strength statistics of either fiber. Specifically, the Weibull modulus determined from the statistics of fracture at one gauge length cannot be used to determine strength at other gauge lengths or for fibers with different diameters. An examination of the literature for ceramic fibers finds that large differences in Weibull modulus for the gauge length and strength distribution technique are common. The Weibull modulus has been determined to be a factor of 2 higher with the gauge length technique than the strength distribution technique for Fiber FP and PRD-166 [15], Nicalon [13], and carbon fibers [24,25]. The reason for this phenomenon is not fully understood. However, some speculation on possible causes may be useful.

It is not commonly understood that fiber diameter variability will have an effect on measured Weibull modulus. Weibull theory predicts that fibers with larger diameter should, on average, have a greater chance to have a large flaw, and will therefore be weaker than smaller fibers. This is well understood. However, for fiber testing, it has special relevance. Because there is a distribution of individual fiber diameters within a tow, the tested volume will vary even when the tested gauge length is constant. Thus, the measured strength distribution will be created by the overlap of the dispersion of strength due to the volumetric distribution of flaws and due to the variable fiber volume. Because of this effect, the natural distribution of fiber strength will be artificially broadened, lowering the measured Weibull modulus. Initially, it was suspected that the measured Weibull modulus of 12 for Nextel 610™ fibers at 25 mm gauge length could have resulted from the combined effect of a gauge length Weibull modulus of 22 with a diameter Weibull modulus of 3. To determine the viability of this hypothesis, a few simple calculations were made. The width of overlapping distributions can be calculated using the following equation:

$$CV_{total}^2 = CV_1^2 + CV_2^2 \qquad (10)$$

Where CV_1 and CV_2 are the coefficient of variations of population 1 and 2, respectively. For Nextel 610™ fibers, the coefficient of variation in fiber diameter was 0.046. This is equivalent to a 9.4% variation in volume. For a

Weibull modulus (relative to diameter variation) of 3, Equation 5 predicts a change in strength of 3.0% for a 9.4% change in volume. For m = 22, the CV will be 0.0545 (from Eq. 9). Combining the CVs with Eq. 10, the measured CV would be $(0.0545^2 + 0.03^2) = 0.0624$, equivalent to m = 19.2. This is a change of 13% from the "true" value of 22. However, it does not accurately predict the measured value of 12. Therefore, this effect does not explain the observed results. Note, however, that this effect could become quite important if the diameter variability were larger. The diameter distributions of other ceramic fibers can be as much as 15% [9,13]. For a diameter CV of 0.15, the combined Weibull modulus using m = 3 and 22, as above, would be $(0.0545^2 + 0.0976^2) = 0.112$. This is equivalent to m = 10.7, or only about 50% of the "true" Weibull modulus. This is a significant change.

An initial attempt to treat this effect analytically was made by Wagner [26,27]. A three-parameter model for Weibull modulus using an additional parameter δ to take into account the effect of fiber diameter was proposed:

$$P = 1-\exp[-(D/D_o)^{\delta}(\sigma/\sigma_o)^m] \qquad (11)$$

Where δ is a parameter similar to Weibull modulus and D_o is a scaling parameter. Wagner assumed that the parameter δ was equal to 2/m, as predicted by the Weibull equations for volume flaws. This equation was also used by Masson [20]. In that study, δ was allowed to take any value; it was found that δ

was typically as large or larger than m, but the scatter was also large. However, in both cases, Equation 10 was found to provide improved fit to the experimental data. Potentially, this equation could be extended to gauge length variation as well, with a third experimental parameter. However, this would add considerable complication to the Weibull theory. Because of this, and since these effects were not large enough to explain the results with Nextel fibers, no attempt was made to calculate δ in this study.

Diameter measurement error could also produce significant changes in measured Weibull modulus. If, because of measurement errors, some fibers are measured to have smaller diameters than they actually have, erroneously high strength values will be generated. Conversely, erroneously large diameter measurements will produce low strength values. Thus, the consequence of this phenomenon is that the strength distribution at a single gauge length will be broadened, so the Weibull modulus will be underestimated. For instance, a mean diameter measurement error of 5% would produce a CV in area and therefore measured strength, of 10.25%. Using Equation 9, a CV in strength of 0.1025 corresponds to a Weibull modulus of 11.7. Thus, even if the fiber had zero true variability, the Weibull modulus would be less than that measured for Nextel 610. Note that a 5% error in diameter measurement represents only 0.6 µm for a 12 µm diameter fiber. Given that most fiber diameter measurements are done using optical microscopes, this magnitude of error would not be unexpected, unless special precautions are taken. Thus, extreme care must be taken to minimize diameter measurement error. In this study, the measurement error was 0.1%. This would produce a CV in strength of 0.0175. If the true Weibull modulus was 22, the combined CV would be $(0.0545^{2} + 0.0175^{2}) = 0.0572$, equivalent to m = 21.0. This is only 5% less than the Weibull modulus in the absence of measurement errors. Therefore, measurement error is not sufficient to explain the observed differences in Weibull modulus.

If we assume that measurement error is not a factor, and diameter variability is not large enough to explain the differences in measured Weibull modulus, then what physical phenomenon could cause the Weibull modulus to be largest with respect to gauge length variability, intermediate for the strength distribution, and smallest for the diameter variability? This result suggests that the flaw population is not random, but that 1) there are, on average, larger flaws in large diameter fibers than predicted from their increased volume, and 2) there is a broader flaw distribution between different fibers in a tow than the distribution of flaws down the length of a single fiber. Considering situation 1), there are several reasons why fiber diameter would be expected to have a stronger than predicted effect on strength than gauge length. Experiments with large diameter Nextel™ 610 fibers for titanium and intermetallic composites have demonstrated that it is difficult to produce large diameter fibers using the Nextel™ process. High strength continuous fibers with diameters as large as 20 µm have been produced [28], but significant process changes were required. If these processes are not performed correctly, critical defects, such as welds, blisters and voids, were created during processing. In a single tow, all fibers are processed at identical conditions. Thus, the larger fibers in the tow may have a larger probability of incurring process-related damage than the smaller fibers. This would produce the low Weibull modulus as measured by the diameter variability method. However, note that the observed flaws in these fibers were primarily welds, which are not related to pyrolysis problems (see below).

Situation 2, the prediction of variation in flaw population between different fibers, is illustrated in Figure 9. In this scenario, each fiber would have a separate and unique population of flaws. Some fibers would have a distribution of relatively small flaws. Some fibers would have a distribution of larger flaws. Thus, if one separated a number of fibers from the bundle and tested them, one would get a wide strength distribution (and therefore low Weibull modulus), since the flaw size on different fibers would be quite different. However, if one tested fibers at different gauge lengths, the result would be a high Weibull modulus. This is true since this measurement would have not be related to the distribution of flaw size between fibers, but would correspond to the distribution of flaws within individual fibers. The wide strength distribution between fibers would be lost, since the mean strength at each gauge length, rather than the distribution of strength, would be used for the analysis. The Weibull modulus as determined from the strength distribution at a single gauge length would have an intermediate value. This physical model would explain the observed results for Nextel™ 610 and 720 fibers.

The question then arises: is there a plausible physical basis for this scenario? The most common cause of fracture in Nextel™ 610 and 720 fibers are weld lines. Figure 10 shows a Nextel™ 610 fiber with fracture originating at a weld line (fracture stress = 2960 MPa). These are believed to result from contact between adjacent fibers during processing, possibly during sintering. The size of the flaws is typically < 0.5μm, as expected by simple calculation from the Griffith fracture criterion using K_{Ic} = 4 for alumina. For fibers to form welds, they must obviously be in contact with adjacent fibers. In a tow of 420 filaments, it would be expected that some filaments would be touching and some would not. For instance, the opportunities for fibers on the outside of the tow to touch neighbors is less than in the center of the bundle. The severity of the weld would then vary between fibers within a bundle. Conversely, the weld line may produce a very narrow distribution of flaws down the length of the fiber. Of course, for any given fiber, the weld tracks may start and stop at various points down the length of the fiber. However, within the gauge length examined in this study, welding may be consistent down the length of the fiber. Thus, it seems possible that the scenario of Figure 9 may occur.

In earlier-generation Nextel™ 610 fibers, in addition to lower Weibull modulus, the gauge length and standard deviation methods produced equal results [10]. However, this fiber had a different type of fracture origins [29]. Although welds were also observed, particulate inclusions originating as contaminants in the fiber precursor were a primary cause of fracture. In this case, defects would be expected to be distributed randomly in the volume of the fibers, since each particle would have an equal chance of being incorporated into any fiber. This creates a situation where the Weibull theory, which assumes a random distribution of flaws within the volume of the samples, is accurate. Thus, even for a single fiber type such as Nextel™ 610, it is difficult to have a high degree of confidence in extrapolating Weibull parameters without extensive test data, including a detailed knowledge of the fracture origins. Perhaps it is not surprising that the fracture statistics change with process modifications; however, this illustrates the difficulty in using Weibull theory for mechanical property prediction. Certainly, using Weibull theory without considering the nature of the flaw distributions can lead to an incorrect extrapolation of fiber properties.

5. Conclusions

The tensile strength of Nextel™ 610 and Nextel™ 720 fibers was determined to be 3200 and 2100 MPa, respectively. The high strength and narrow strength distribution of Nextel™ 610 was attributed to a reduction in flaw size due to process improvements.

The Weibull modulus of both fibers was measured using three different techniques. The Weibull modulus of Nextel™ 610 and Nextel™ 720 fibers was 22 and 26, respectively, when determined from the variability with changing gauge length, 11.5 and 8, respectively, when determined from strength variability at a single gauge length, and 3.1 and 2.8, respectively, when determined from variability between fibers with different diameter. Thus, traditional two-parameter Weibull statistics were not sufficient to describe the fracture statistics of Nextel™ 610 and Nextel™ 720 fibers. Mechanisms for non-random fiber flaw generation during fiber processing were proposed to explain the measured effects.

The high Weibull modulus with respect to strength variability and gauge length variation indicates the degree of consistency achieved during fiber processing. The effect of the low Weibull modulus with respect to diameter variation is of minor practical importance because the diameter size variability was small.

Acknowledgments

The assistance of Dave Lueneburg, Steve Lieder, and Margaret Vogel-Martin in fiber test development as well as Dave Jensen and Robinson Vo at 3M and Alan Seid and Christy Schramm at Touchstone Research Laboratories in fiber testing is gratefully appreciated.

References

1. H.E. DEVE and C. McCULLOUGH, *J. of Met.*, **47** (1995) 33-37 .

2. D.M. WILSON, D.C. LUENEBURG, and S.L. LIEDER, *Ceram. Eng. Sci. Proc.*, **14** (1993) 609-621.

3. D.M. WILSON, S.L. LIEDER, and D.C. LUENEBURG, Materials Research Society Symposium Proceedings, Vol. 350, Intermetallic Matrix Composites III, edited by J.A. Graves, R.R. Bowman, and J.J. Lewandowski (Mat. Res. Soc., Pittsbury, PA, 1994) pp. 89-98.

4. D.M. WILSON, S.L. LIEDER, and D.C. LUENEBURG, *Cer. Eng. Sci. Proc.*, **16** (1995) 1005-1014.

5. S. VAN DER ZWAAG, *J. Test Eval.*, **17** (1989) 292-298.

6. A. KELLY and N.H. MACMILLAN, "Strong Solids", 3rd ed. (Clarenden Press, Oxford, 1986).

7. B. BERGMAN, *J. Mat. Sci. Ltrs.*, **5** (1986) 611-614.

8. J. K. WEDDELL, *J. Text. Inst.*, **81** (1990) 333-59.

9. B. BERGMAN, *J. Mat. Sci. Ltrs.*, **3** (1984) 689-692.

10. M.M. VOGEL-MARTIN and D.M. WILSON, NASA Conf. Publ. 3175, part 2, 1992, 16th Annual Conference on Metal Matrix Carbon and Ceramic Matrix Composites, pp. 519-533.

11. H.F. WU and A.N. NETRAVALI, *J. Mat. Sci.*, **27** (1992) 3318-3324.

12. Y. MATSUO, J.X. LI, and S. KIMURA, *Adv. Comp. Mat.*, **2** (1992) 17-28.

13. G. SIMON and A.R. BUNSELL, *J. Mat. Sci.*, **19** (1984) 3649-3657.

14. J. NUNES, *Comp. Techn. Rev.*, **5** (1983) 53-60.

15. V. LAVASTE, J. BESSON, and A.R. BUNSELL, *J. Mat. Sci.*, **30** (1995) 2042-2048.

16. S.N. PATANKAR, *J. Mat. Sci. Ltrs.*, **10** (1991) 1176-1181.

17. Ch. LESNIEWSKI, C. AUBIN, AND A.R. BUNSELL, *Comp. Sci. and Tech.*, 37 (1990) 63-78.

18. K. JAKUS and V. TULLURI, *Ceram. Eng. Sci. Proc.*, **10** (1989) 1338-1349.

19. Y. TANABE, E. YASUDA, and A.R. BUNSELL, Y. Favry, M. Inagaki, and M. Sakai, *J. Mat. Sci.*, 26 (1991) 1601-1604.

20. J.J. MASSON, K. SCHULTE, F. GIROT, and Y. LE PETITCORPS, *Mat. Sci. Eng.*, **A135** (1991) 59-63.

21. S-H. OWN, R.V. SUBRAMANIAN, and S.C. SAUNDERS, *J. Mat. Sci.*, 21 (1986) 3912-3920.

22. J. BREEDON JONES, J.B. BARR, and R.E. SMITH, *J. Mat. Sci.*, 15 (1980) 2455-2465.

23. Z.R. XU, K.K. CHAWLA, and X. LI, *Mat. Sci. Eng.*, **A171** (1993) 249-256.

24. El.M. ASLOUN, J.B. DONNET, G. GUILPAIN, M. NARDIN, and J. SCHULTZ,*J. Mat. Sci.*, 24 (1989) 3504-3510.

25. J.W. HITCHON and D.C. PHILLIPS, *Fiber Sci. and Tech.*, **12** (1979) 217-233.

26. H. D. WAGNER, S. L. PHOENIX, and P. SCHWARTZ, *J. Comp. Mat.*, **18** (1984) 312-338.

27. H.D. WAGNER, *J. Poly. Sci.: Part B: Polymer Physics*, **27** (1989) 115-149.

28. M.A. LEITHEISER and D.M. WILSON, Alumina Fiber Development NASP Materials/Structures Maturation Program, Phase II Final Report, February, 1991.

29. D. M. WILSON, NASA Conference Proc. 3097, Part 1, 14th Annual Conference on Metal Matrix Carbon and Ceramic Matrix Composites, edited by J. Buckley. pp 105-117.

Table 1. Nextel™ 610 and 720 Fiber Properties

Composition (wt%)	99% Al_2O_3	85% Al_2O_3 + 15% SiO_2
Crystal Structure	α-Al_2O_3	α-Al_2O_3 + mullite
Elastic Modulus (GPa)	380	260
Diameter (µm)	11.5	12.5
Density (g/cm^{3})	3.9	3.4
Creep Rate (1/sec) (1100 C/70 MPa)	1 x 10^{-7}	<1 x 10^{-10}

Table 2. Nextel™ 610 and 720 Fiber Tensile Data

Nextel™ 610 Fiber (A0168)			Nextel™ 720 Fiber (A0172)		
Load (g)	Fiber Dia. (µm)	Strength (MPa)	Load (g)	Fiber Dia. (µm)	Strength (MPa)
28.5	11.0	2944	26.4	12.3	2199
32.8	11.3	3206	26.3	12.3	2185
32.3	12.1	2751	22.6	12.3	1882
31.6	11.3	3089	23.3	11.1	2358
33.0	11.0	3406	22.5	11.1	2282
32.9	11.2	3275	24.6	11.6	2282
27.6	11.5	2606	26.4	12.3	2192
29.3	11.6	2723	21.4	12.4	1744
25.3	11.3	2475	23.1	11.8	2061
28.9	11.1	2930	21.1	12.6	1648
26.8	11.5	2530	26.6	12.1	2261
27.2	11.9	2399	20.1	12.4	1641
33.4	12.2	2806	22.3	12.1	1896
32.1	11.9	2827	24.1	12.5	1923
30.2	11.3	2951	21.0	11.9	1861
26.2	10.7	2854	23.9	12.5	1903
28.4	11.0	2930	21.5	12.0	1868
25.8	11.2	2565	16.6	12.0	1441
27.6	11.1	2799	23.7	11.9	2096
30.1	11.0	3102	26.6	12.3	2213
36.6	11.5	3454	22.9	12.9	1717
40.6	11.0	4185	25.5	12.7	1972
35.1	11.9	3095	22.1	12.9	1655
29.2	10.6	3247	22.8	13.0	1682
30.9	10.7	3371	27.6	12.5	2206
34.4	11.4	3302	21.5	12.8	1641
36.2	11.3	3544	19.2	12.8	1462
38.5	11.8	3454	15.9	12.7	1234
39.3	11.9	3468	20.9	13.5	1434
35.5	11.7	3233	31.4	12.7	2434
32.2	12.5	2571	23.1	11.8	2068
29.4	10.6	3268	19.1	11.3	1868
28.6	11.3	2792	22.3	12.0	1937
33.6	12.0	2916	26.9	13.1	1958
29.7	11.1	3006	25.9	12.1	2206
33.5	10.9	3523	24.1	11.8	2158
26.6	10.6	2958	25.4	11.9	2241
29.7	10.9	3123	26.1	11.5	2468

	26.9	10.7	2930	19.8	11.6	1841
	25.1	10.8	2689	19.8	11.6	1834
	34.9	11.9	3075	24.6	12.7	1903
	33.5	11.2	3337	26.0	12.2	2179
	37.4	11.6	3468	25.8	12.7	1999
	30.4	10.8	3254	20.9	12.6	1641
	39.5	12.7	3061	26.7	12.4	2165
	32.2	10.5	3647	35.0	13.6	2365
	29.1	10.5	3295	19.8	11.5	1868
	31.5	11.5	2971	25.2	11.7	2296
	33.1	11.6	3068	19.3	12.1	1648
	31.5	10.8	3371	26.8	12.4	2179
Mean	31.5	11.3	3077	23.5	12.2	1964
St. Dev.	3.88	0.52	348	3.46	0.56	287
CV	0.123	0.046	0.113	0.147	0.045	0.146

Table 3. Weibull Properties of Nextel™ 610 fiber

		Weibull Modulus Calculation		
Lot	Mean Strength MPa	Strength Distribution	Diameter Distribution	Gauge Length Dependence
A0168	3080	10.9	2.7	-
A0180	3030	11.2	2.6	-
A0184	3500	12.1	4.0	-
mean	3200	11.4	3.1	21.7

Table 4. Weibull Properties of Nextel™ 720 fiber

		Weibull Modulus Calculation		
Lot	Mean Strength MPa	Strength Distribution	Diameter Distribution	Gauge Length Dependence
A0080	2130	7.1	4.0	-
A0174	2030	8.1	1.6	26.4
mean	2080	7.6	2.8	-

Figure 10. Scanning electron micrograph of Nextel™ fiber showing weld line at fracture origin (fracture stress = 2960 MPa).

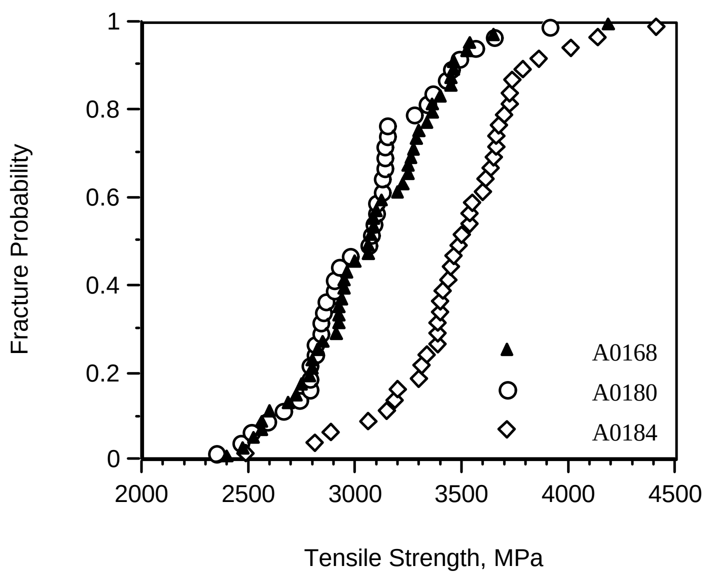

Figure 1. Fracture probability of 3 lots of Nextel™ 610 fiber

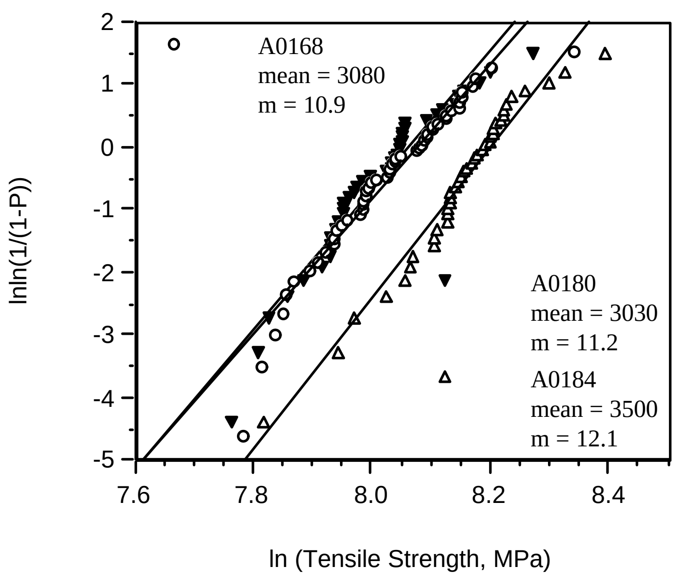

Figure 2. Weibull plot for 3 lots of Nextel™ 610 fiber

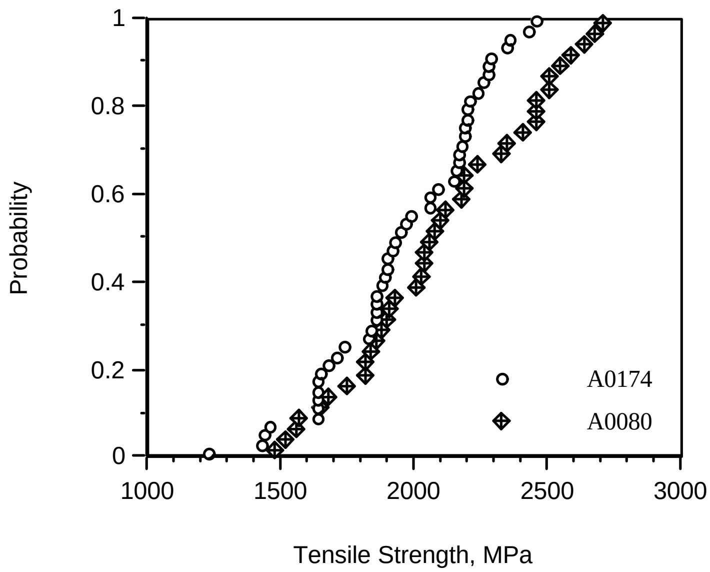

Figure 3. Fracture probability for 2 lots of Nextel™ 720 fiber

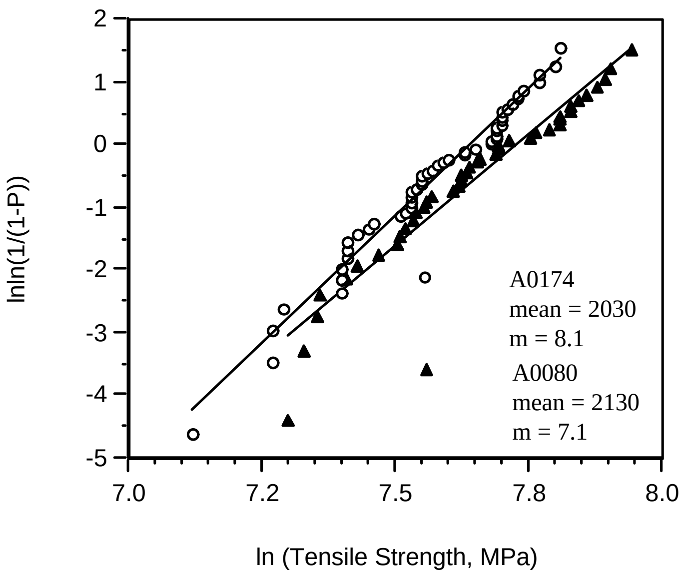

Figure 4. Weibull plot for 2 lots of Nextel™ 720 fiber

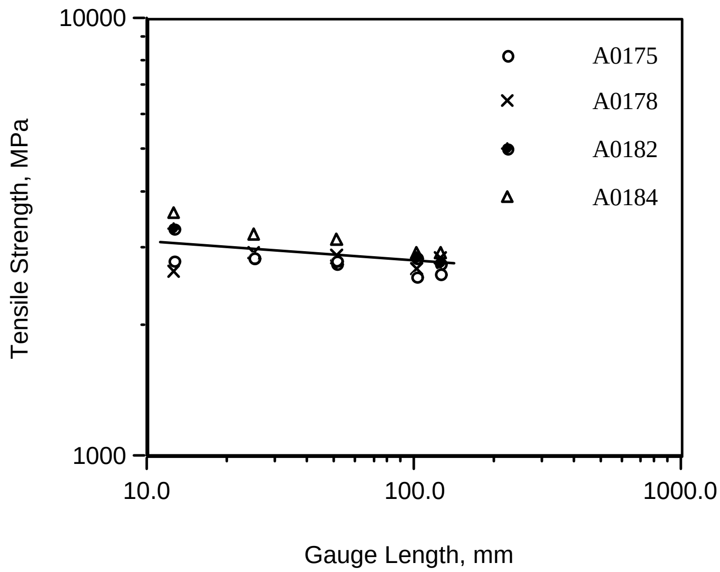

Figure 5. Tensile strength of 4 lots of Nextel™ 610 fiber as a function of gauge length. The line is the least squares fit of the mean strength of all 4 lots.

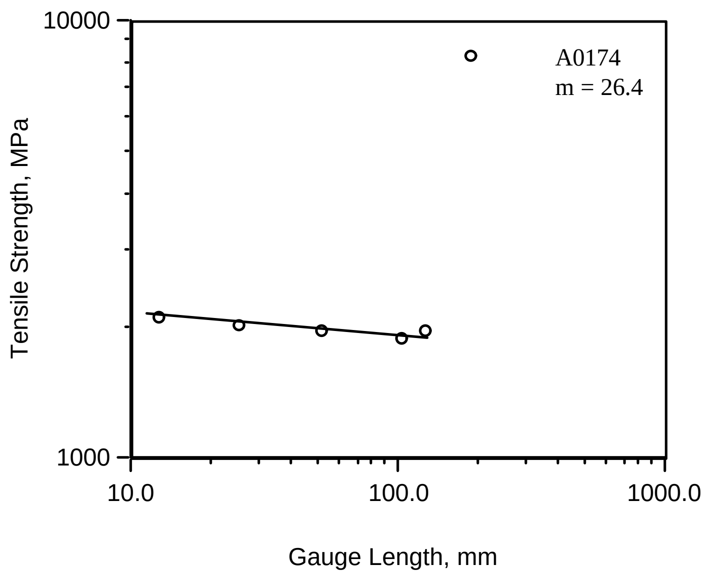

Figure 6. Tensile strength Nextel™ 720 fiber as a function of gauge length.

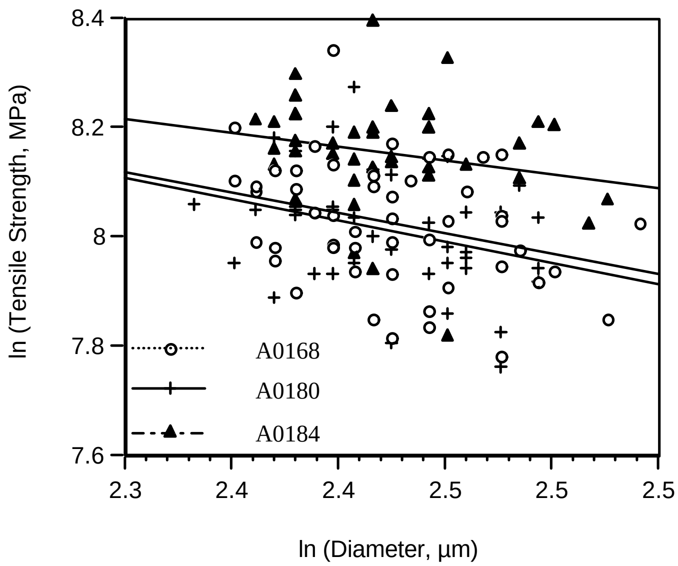

Figure 7. Tensile strength of 3 lots of Nextel™ 610 fiber as a function of fiber diameter.

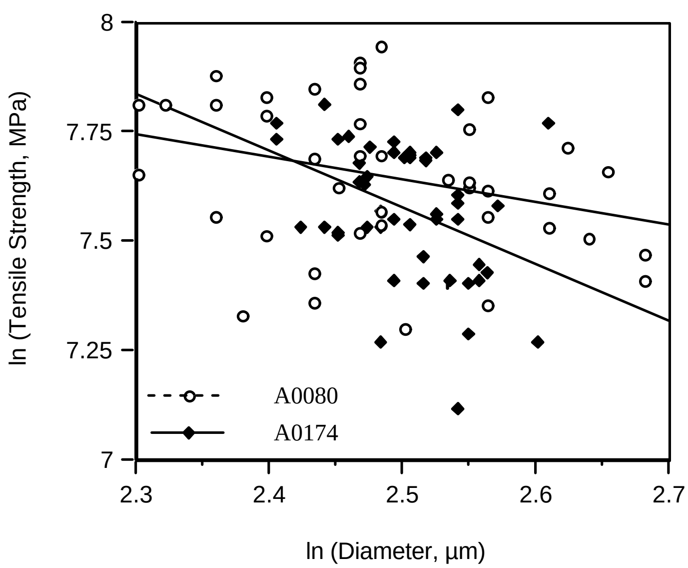

Figure 8. Tensile strength of Nextel™ 720 fiber as a function of fiber diameter.

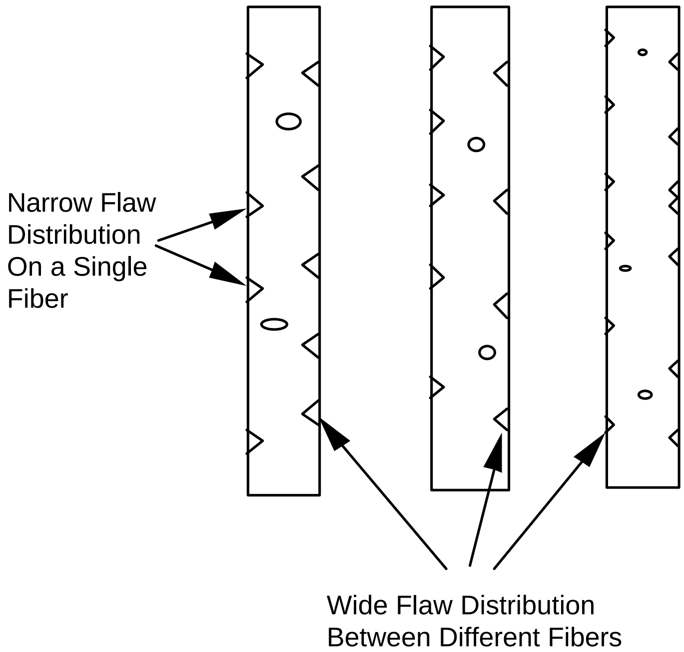

Figure 9. Schematic flaw size distributions. Some fibers have larger flaws than others, but the size distribution is narrow for individual fibers.

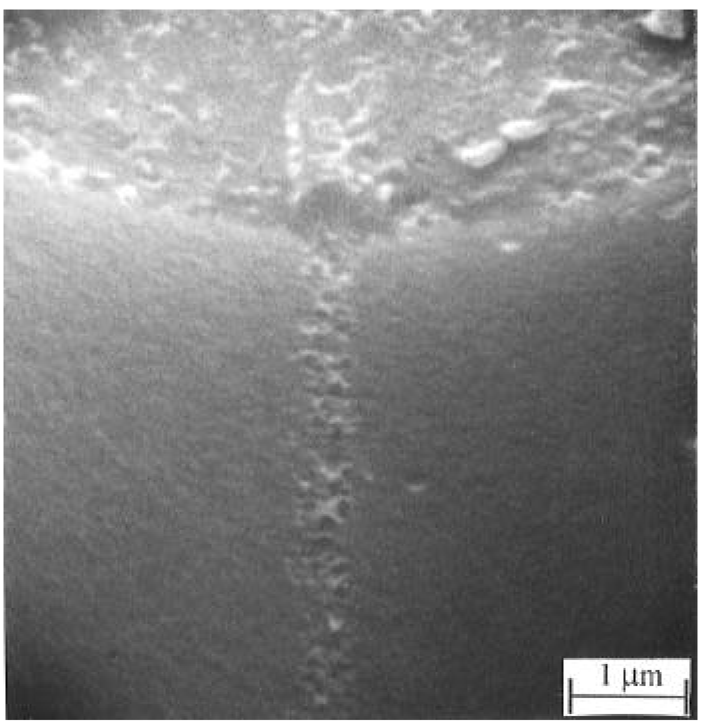

Figure 10. Scanning electron micrograph of Nextel™ fiber showing weld line at fracture origin (fracture stress = 2960 MPa).